Nonlocal Constitutive Relation for Steady Granular Flow

Ken Kamrin[1,*] and Georg Koval[2]

[1]Department of Mechanical Engineering, MIT, Cambridge, Massachusetts 01239, USA

[2]Laboratory of Engineering Design, National Institute of Applied Sciences, Strasbourg, France

(Received 4 January 2012; revised manuscript received 22 February 2012; published 26 April 2012; corrected 1 May 2012; corrected 7 August 2014)

Extending recent modeling efforts for emulsions, we propose a nonlocal fluidity relation for flowing granular materials, capturing several known finite-size effects observed in steady flow. We express the local Bagnold-type granular flow law in terms of a fluidity ratio and then extend it with a particular Laplacian term that is scaled by the grain size. The resulting model is calibrated against a sequence of existing discrete element method data sets for two-dimensional annular shear, where it is shown that the model correctly describes the divergence from a local rheology due to the grain size as well as the rate-independence phenomenon commonly observed in slowly flowing zones. The same law is then applied in two additional inhomogeneous flow geometries, and the predicted velocity profiles are compared against corresponding discrete element method simulations utilizing the same grain composition as before, yielding favorable agreement in each case.

DOI: 10.1103/PhysRevLett.108.178301 PACS numbers: 47.57.Gc, 45.70.Mg, 83.10.Ff, 83.80.Fg

In homogeneous, steady, 2D simple shearing of a granular material composed of stiff frictional disks, a local rheology emerges of the form $\mu = \mu(I)$ in accord with dimensional arguments, where $\mu = \tau/P$ for shear stress τ and normal pressure P, and I is the inertial number $\dot{\gamma}\sqrt{m/P}$ for particle mass m. In simulations of da Cruz *et al.* [1], the law was quantified and found to be roughly linear, inverted to read

$$I(\mu) = H(\mu - \mu_s)(\mu - \mu_s)/b \tag{1}$$

for constant b and static yield coefficient μ_s and Heaviside function H. By isotropic extension, it has been generalized to a three-dimensional form for arbitrary flows and proven effective in certain geometries [2,3].

Nonlocal effects cause divergence from the above law and are most commonly studied in two senses. (i) In inclined plane flow, thin granular layers (measured in terms of d, the particle diameter) require a higher angle of incline before flow ensues. Since μ is uniform in this geometry, internal strength μ_s could be deemed thickness-dependent in thin granular layers [4] (a property also observed in suspensions [5]). (ii) In large bodies of granular material undergoing steady inhomogeneous deformation, the local law predicts zero flow in regions where $\mu < \mu_s$. However, this is not what is observed; "subyield" regions of $\mu < \mu_s$ commonly possess slow flowing material, and the shear-rate profile therein has an exponentially decaying character with decay length scaled by the grain diameter [6,7]. It is also observed that shear rate becomes independent of the stress in these quasistatic zones, which defies the clear rate dependence of the local law [8].

In this Letter, we propose and directly test a partial differential equation (PDE) nonlocal flow rule for granular materials aimed at describing steady-flow nonlocality, sense (ii) above. The key novelty of the approach is its geometric generality, quantitative predictability, and its ability to bridge in one simple form the inertial regime with the quasistatic, including the onset of rate independence and finite-size effects. The model is obtained by extending the nonlocal fluidity approach of Ref. [9], originally used for emulsions. Integral equations have also been used describe nonlocal flow, as in Ref. [10], and can explain sense (i) nonlocality as an effect of a thin domain of integration. On the other hand, a simpler PDE-based rheology can be derived as the "large-domain" limit of an integral law, obtained by integrating over all space after Taylor expanding the integrand. Past PDE-based laws include the theory of partial fluidization [11], kinetic fluctuational theory [12], and the stochastic flow rule [13]. Since nonlocal effects are dominant in slowly flowing zones, the data against which we test our model must be obtained down to very small flow rates, and success is measured by agreement over the entire range of rates. Discrete particle simulations for three different geometries (see Fig. 1) are used for model validation, which can be accurately discerned down to almost arbitrarily small flow rates.

The existing model of nonlocal fluidity for a pressure-insensitive emulsion, flow varying only in z, is as follows. Define the fluidity by $f = \dot{\gamma}/\tau$, equivalent to the inverse viscosity. In a homogeneous flow, a known local rheology $\dot{\gamma} = \dot{\gamma}(\tau)$ is obeyed. Thus, $f = f_{\mathrm{loc}}(\tau) = \dot{\gamma}(\tau)/\tau$. If the local law has a yield stress τ_y, then $f_{\mathrm{loc}}(\tau < \tau_y) = 0$. The internal length scale causes the fluidity to be affected by plastic rearrangements nearby. Thus, by defining ξ as the corresponding "cooperativity length" of the plastic deformation mechanism, the fluidity is set to obey

$$f - f_{\mathrm{loc}}(\tau) = \xi^2 \partial^2 f/\partial z^2. \tag{2}$$

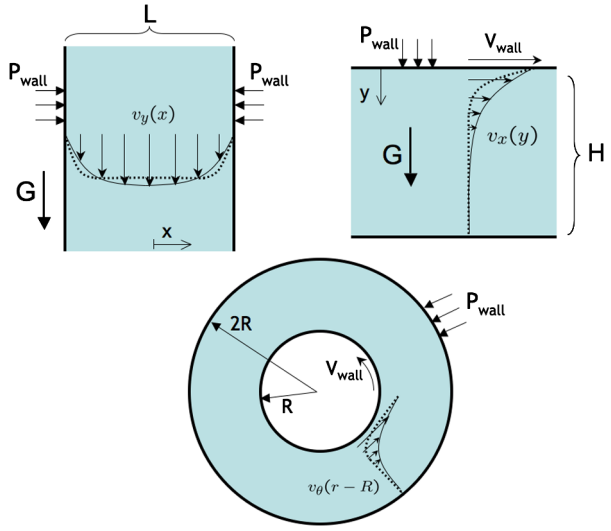

FIG. 1 (color online). Geometries being considered, with qualitative depictions indicating the contrast between observed velocity fields (vectors and solid lines) and predictions of the local flow law Eq. (1) (dotted lines).

For a known stress field $\tau(z)$, the full flow solution is given by solving the above and then substituting the solution into $\dot{\gamma}(z) = \tau(z)f(z)$ to obtain the flow profile. The law is similar to an inhomogeneous Helmholtz equation, which naturally "diffuses" any sharp flow cutoffs in the f_{loc} field into exponential-type decay in the f field.

However, an equally important (though less appreciated) feature is that the fluidity becomes completely rate-independent whenever f_{loc} vanishes. Hence, in regions where $\tau < \tau_y$, the law reduces to $f - \xi^2 \partial^2 f/\partial z^2 = 0$, a linear ordinary differential equation with the property that if $f(z)$ solves the system, so does $\alpha f(z)$ for any scalar α. Consequently, $\dot{\gamma}(z)$ can be scaled by any multiple, regardless of the stress magnitude, and remain a valid solution. This property characterizes rate independence. Furthermore, the second-order term implies that shear bands never shrink below a finite width governed geometrically by ξ, a well-observed property of steady granular flow. Together with the diffusive character discussed above, the nonlocal fluidity model becomes attractive to adapt for granular materials modeling.

Let us define the "granular fluidity" by

$$g = \frac{\dot{\gamma}}{\mu} \rightarrow g_{\mathrm{loc}}(\mu, P) = H(\mu - \mu_s)\frac{\mu - \mu_s}{b\mu}\sqrt{\frac{P}{m}}; \quad (3)$$

the latter follows from the local law previously discussed. We keep the numerator as $\dot{\gamma}$, because, as discussed in the theory of fluidity, it must give the time scale of macroscopic deformation; however, the denominator is switched to μ, because the friction state now determines closeness to yielding.

For a quantitative description of ξ, we look to the next advancement in nonlocal fluidity theory [14], which derives ξ as a function of the stress state based on the notion that plastic rearrangements induce stress redistribution (a mechanical picture common to other nonlocal approaches including Ref. [10]). We adopt their framework by replacing τ with μ accordingly, leaving the general form

$$\xi = \xi(\mu) = A\left(\frac{1 + H(\mu_s - \mu)}{|\mu - \mu_s|}\right)^{\alpha} d \quad (4)$$

for A a dimensionless scaling constant and d the microlength size (the grain width in our case). The divergence of ξ approaching the yield point is validated by multiple amorphous matter studies [15–17]. Our discrete element method (DEM) data also support this point, as we will see momentarily.

As in Ref. [14], the Laplacian can be used to generalize the nonlocal law to two spatial dimensions. Hence,

$$\nabla^2 g = \frac{1}{\xi^2}(g - g_{\mathrm{loc}}). \quad (5)$$

Similarly, we generalize to planar tensorial definitions of the scalar quantities: $\dot{\gamma} = \sqrt{2\sum D'_{ij}D'_{ij}}$, $P = -\frac{1}{2}\,\mathrm{tr}(\boldsymbol{\sigma})$, and $\mu = \sqrt{0.5\sum \sigma'_{ij}\sigma'_{ij}}/P$ for strain-rate tensor $\mathbf{D} = 0.5[\nabla\mathbf{v} + (\nabla\mathbf{v})^T]$ and Cauchy stress $\boldsymbol{\sigma}$, and $'$ means the deviatoric part. For now, we study only geometries whose steady flow is incompressible: $\mathrm{tr}\mathbf{D} = 0$.

Interestingly, Eq. (5) has certain similarities with the law governing the order parameter ρ in steady-state partial-fluidization theory. Both have a Laplacian term, but in the latter the remaining terms are nonlinear, which prevents direct quasistatic rate independence but allows certain dynamical phenomena in its full form, such as stick-slip behavior. It should also be pointed out that newly developed implicit gradient plasticity models have also exploited a state variable obeying a law like Eq. (5) but with "fictitious plastic strain" replacing the fluidity [18].

Our model [Eqs. (3)–(5)] requires four total modeling parameters to characterize the granular matter. We use $b = 1.05$ and $\mu_s = 0.26$ from existing planar shear data utilizing the same DEM disk properties. While the theory for emulsions gives $\alpha = 0.5$, we find that $\alpha = 0.6$ gives a better fit to data and shall use this number. We also find $A = 0.31$ to be a good choice. These numbers are used for *all* calculations in this Letter. We check our model against DEM simulations, which follow the same scheme precisely described in Ref. [8]; the material is composed of $\pm 20\%$ polydisperse disks with mean diameter d, mean mass m, surface friction $\mu_c = 0.4$, contact elastic stiffnesses $k_n \geq 10^4 P$ (corresponding to stiff particles), $k_t = 0.5k_n$, and restitution coefficient $e = 0.1$.

We use MATHEMATICA 10 to compute high-precision numerical solutions for the model, straightforward because the model reduces to an ordinary differential equation in spatially symmetric geometries as we consider here. The geometries we consider have simple stress fields, which we

use as the input to solve for g. In the DEM simulations, the velocity of the wall and that of the free material adjacent to it are frequently mismatched due to imperfections in attaining a fully rough condition, so, while we use the V_{wall} as a reference value, our actual PDE boundary values utilize that of the adjacent mobile material and not the wall itself. Because of the immobility of wall particles, we postulate that granular fluidity at the boundaries g_{wall} is a function of the local stress state and have found $g_{\text{wall}} = g_{\text{loc}}$ to be appropriate for fully rough walls (as in Refs. [9,18,19]) or in general for flows where the inertial number I is large near the walls. However, an in-depth future study is necessary to fully quantify the boundary conditions.

We first test our model rheologically, by comparing against the detailed report by Koval *et al.* [8] for DEM simulations of the annular shear cell. The geometry has two concentric fully rough walls. The inner wall at $r = R$ is rotated at a fixed rate Ω (i.e., $V_{\text{wall}} = R\Omega$), and the outer wall at $r = 2R$ is prevented from rotating but permits some inward wall movement to provide a fixed inward pressure P_{wall} (force per length). In the steady state, moment balance gives $\tau_{r\theta}(r) = S(R/r)^2$ for inner wall shear stress S, and the normal components are observed (through coarse-graining) to obey $\sigma_{\theta\theta}(r) \approx \sigma_{rr}(r) \approx -P_{\text{wall}}$ to a good approximation throughout. Hence we have $P(r) = P_{\text{wall}}$ and $\mu(r) = |\tau_{r\theta}(r)/P_{\text{wall}}|$.

The first data against which we test are a set of steady-flow simulations conducted for different choices of the size ratio $\tilde{R} = R/d$ with fixed normalized inner wall speed $\tilde{V}_{\text{wall}} = V_{\text{wall}}\sqrt{m/(d^2 P_{\text{wall}})} = 2.5$. In each run, when the steady state is reached (taken as $\tilde{V}_{\text{wall}}\Delta t \geq 100$, where Δt is the simulation time), coarse-grained (I, μ) pairs from radial positions r (see [8] for the averaging method) are plotted [see Fig. 2(a)]. For large values of I, the μ vs I data appear to collapse onto a single curve aligned with the local law. For smaller I, the different tests split off from a single curve in a clear fashion, demonstrative of the size effect. The model captures this effect and simultaneously gives the usual local law under homogeneous planar shear conditions, matching data from Ref. [1]. It can be understood that regions of large I tend to the local law because $g \approx g_{\text{loc}} \gg \xi(\mu)^2\nabla^2 g$ in zones of large μ. We plot corresponding velocity profiles in Fig. 3(a). As discussed in Ref. [8], the material far from the inner wall is not yet in the steady state, and hence our velocity predictions are inferiorly limited by the lowest velocity value (in steady-state range) available for each profile.

Another nonlocal aspect is probed by varying $\tilde{V}_{\text{wall}}$ at fixed $\tilde{R} = 50$. The model solutions are plotted against those of the DEM in Fig. 2(b). The DEM results show clear rate independence; as wall speed decreases, a nearly identical range of μ values corresponds to a completely different range of I for each run. Hence, $\mu(r) \to \mu_s(R/r)^2$, below μ_s almost everywhere, while the *scaled* flow rate field $\dot{\gamma}(r)/\dot{\gamma}_{\text{wall}}$ approaches a seemingly fixed, nowhere-vanishing distribution. This result is also outside the realm of local rate-independent models; for example, critical state soil plasticity would require a single μ value in the steady-flowing zones of an annular shear, but here a range of steady μ values is present.

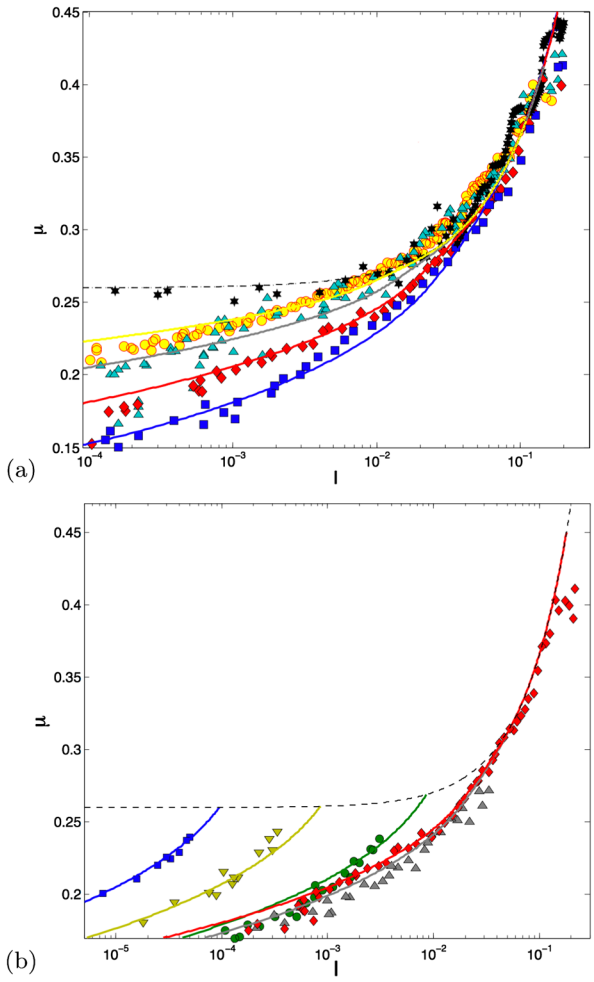

FIG. 2 (color online). μ vs I locus in steady annular shear: (a) Nonlocal model (solid lines) compared to DEM for $\tilde{V}_{\text{wall}} = 2.5$ and $\tilde{R} = 25$ (□), 50 (◇), 100 (△), and 200 (○). (b) Comparisons for fixed $\tilde{R} = 50$ and $\tilde{V}_{\text{wall}} = 0.000\,25$ (□), 0.0025 (▽), 0.025 (○), 0.25 (△), and 2.5 (◇). The local rheology (dotted line) is indicated, to which the nonlocal model approaches only in uniform stress environments [e.g., planar shear, DEM data (★) of Ref. [8]].

With rheological validation in hand, we take the same model, predict flow profiles in different geometries, and compare results to new DEM simulations. In order to decrease the observed disturb of the velocity profiles near the walls, we adopt rough walls composed by particles with a diameter twice as large as the tested material. First, we predict flow in a simple shear geometry with gravity pointing downward, orthogonal to the shear direction. The apparatus has height $H = 40d$, top and bottom rough walls, and periodic boundary conditions on the sides.

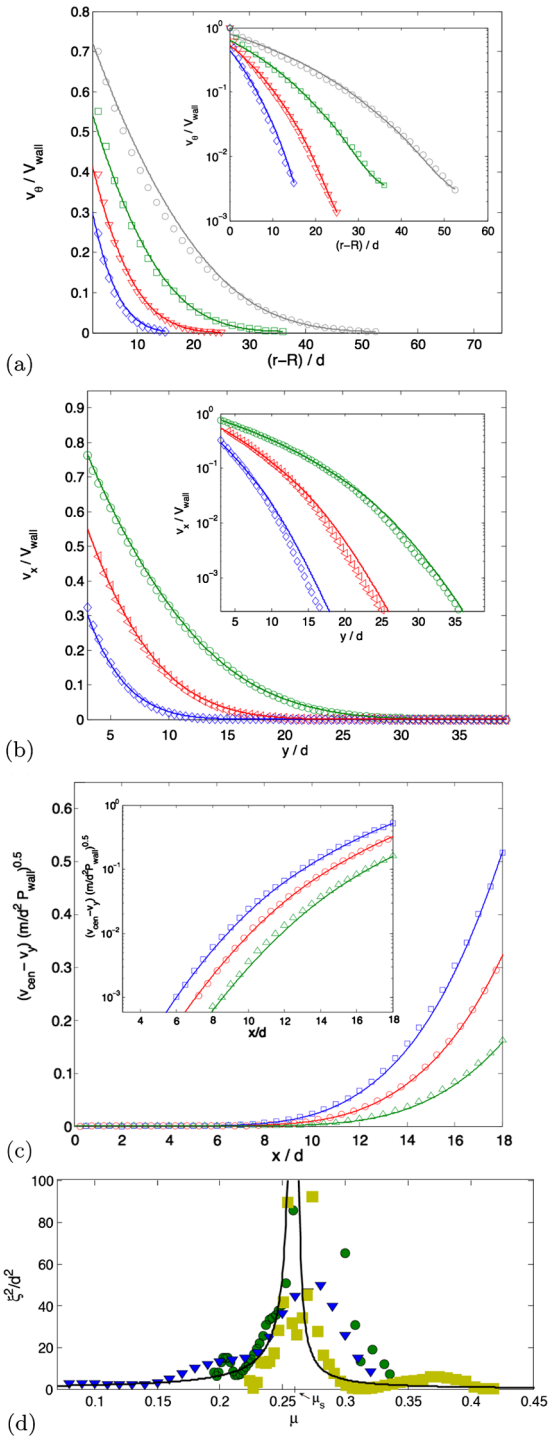

FIG. 3 (color online). (a)–(c) DEM velocity profiles (symbols) vs nonlocal model (solid lines). (a) Annular shearing (DEM data from Ref. [8]): $\tilde{V}_{\mathrm{wall}} = 2.5$ and $\tilde{R} = 25$ ($\diamond$), $\tilde{R} = 50$ ($\triangledown$), $\tilde{R} = 100$ ($\square$), and $\tilde{R} = 200$ ($\bigcirc$). (b) Planar shear with gravity: $\tilde{V}_{\mathrm{wall}} = 2.5$ and $\tilde{w}_g = 0.04$ ($\diamond$), 0.08 ($\triangleleft$), and 0.16 ($\bigcirc$). (c) Vertical chute flow: $\tilde{w}_g = 0.0175$ ($\triangle$), 0.02 ($\bigcirc$), and 0.0225 ($\square$). (d) Direct measurement of ξ^2/d^2 [by Eqs. (3) and (5)] vs μ from the DEM flow profiles in each geometry: Annular shear $\tilde{R} = 50$, $\tilde{V}_{\mathrm{wall}} = 2.5$ ($\triangledown$), shear with gravity $\tilde{w}_g = 0.04$ ($\bigcirc$), and vertical chute $\tilde{w}_g = 0.225$ ($\square$). The solid line shows theoretical result using $\xi(\mu)$ from Eq. (4).

A pressure P_{wall} is applied to the top surface, and the top wall is given a dimensionless lateral velocity of $\tilde{V}_{\mathrm{wall}} = 2.5$. The wall shear stress S induced by the motion sets the shear stress throughout: $\tau_{xy}(y) = S$. If we define a mean solid fraction ν_m, we can define the normalized weight density of the granular media as $\tilde{w}_g = 4mG\nu_m/(P_{\mathrm{wall}}\pi d)$. The vertical compressive stress increases downward due to gravity, giving $\sigma_{yy}(y) = -P_{\mathrm{wall}}(1 + \tilde{w}_g y/d)$. As before in the Couette cell, we assume $\sigma_{yy}(x) \approx \sigma_{xx}(x)$, which turns out to be well matched by the DEM. Likewise, $\mu(y) = S/[P_{\mathrm{wall}}(1 + \tilde{w}_g y/d)]$. We run DEM simulations for different values of $\tilde{w}_g$ (0.04, 0.08, and 0.16). Comparisons between the DEM and nonlocal model's flow fields are presented in Fig. 3(b). Next, we consider gravity-driven flow down a long vertical chute with rough parallel walls. The walls are separated by a distance $L = 40d$, and a wall pressure P_{wall} is applied. The simulation utilizes periodic boundary conditions at the top and bottom of the chute, implying the Janssen limit where stress becomes vertically invariant. Likewise, $\tau_{xy}(x) = P_{\mathrm{wall}}\tilde{w}_g x/d$ by vertical force balance, and, indeed, we see this formula upheld extremely well in the stress field obtained from the DEM simulations. Again, $\sigma_{yy}(x) \approx \sigma_{xx}(x) = -P_{\mathrm{wall}}$, which gives $\mu(x) = |\tau_{xy}(x)/P_{\mathrm{wall}}|$. We solve Eq. (5) as an ordinary differential equation in x given the stress field as determined from the choice of $\tilde{w}_g$. Figure 3(c) demonstrates that the nonlocal model captures the velocity field [displayed relative to the center velocity $v_y(x = 0) = v_{\mathrm{cen}}$] over several orders of magnitude for different values of $\tilde{w}_g$ (0.0175, 0.02, and 0.0225).

While we desire the simplest possible flow relation, quantitative accuracy is lost when assuming $\xi \approx$ const as in Ref. [9]; for any single value, we always find noticeable deviations in the majority of test cases when plotted as in Figs. 3(a)–3(c). Rather, Fig. 3(d) shows the μ-dependent nature of ξ by comparing DEM values inferred by using Eqs. (3) and (5) to the relation in Eq. (4). An empirical fit for $\xi(\mu)$ could be made to match data better for $\mu > \mu_s$; however, this is the inertial range where ξ has minimal effect, and we prefer to keep with Eq. (4) for its connection to existing theory. Also, in view of our observation that steady-flow normal stresses along and perpendicular to the shear plane are approximately equal (also observed in Refs. [1,20]), it seems that the most general form would be to append the coaxial flow condition $\mathbf{D}/|\mathbf{D}| = \boldsymbol{\sigma}'/|\boldsymbol{\sigma}'|$ to the system, which closes the system of equations for arbitrary geometries. Solutions could be computed by including a small elastic component to the deformation and going to the steady state with an elastoplastic finite-element solver, as done in Ref. [3], with g added as a nonlocal state variable. We should also point out that, in focusing on the steady state, we leave out a description of possible transient behavior; an unsteady version of Eq. (5) ought to include a term proportional to $\dot{g}$, in line with other

approaches to nonlocal flow [11]. A study of the relationship between the grain properties and the nonlocality parameters would be interesting future work. Last, this model treats packing fraction ϕ as a "slave variable," because, in the steady state, the work of Ref. [1] shows $\phi = \phi(I)$ even in inhomogeneous flow geometries [8]. However, for transient analysis, a correct update of ϕ and its effect on μ_s would be necessary.

*kkamrin@mit.edu

[1] F. da Cruz, S. Emam, M. Prochnow, J. Roux, and F. Chevoir, Phys. Rev. E **72**, 021309 (2005).
[2] P. Jop, Y. Forterre, and O. Pouliquen, Nature (London) **441**, 727 (2006).
[3] K. Kamrin, Int. J. Plast. **26**, 167 (2010).
[4] L. E. Silbert, J. W. Landry, and G. S. Grest, Phys. Fluids **15**, 1 (2003).
[5] C. Bonnoit, T. Darnige, E. Clement, and A. Lindner, J. Rheol. **54**, 65 (2010).
[6] G. D. R. Midi, Eur. Phys. J. E **14**, 341 (2004).
[7] D. M. Mueth, Phys. Rev. E **67**, 011304 (2003).
[8] G. Koval, J.-N. Roux, A. Corfdir, and F. Chevoir, Phys. Rev. E **79**, 021306 (2009).
[9] J. Goyon, A. Colin, G. Ovarlez, A. Ajdari, and L. Bocquet, Nature (London) **454**, 84 (2008).
[10] O. Pouliquen and Y. Forterre, Phil. Trans. R. Soc. A **367**, 5091 (2009).
[11] I. S. Aranson and L. S. Tsimring, Phys. Rev. E **64**, 020301 (2001).
[12] S. B. Savage, J. Fluid Mech. **377**, 1 (1998).
[13] K. Kamrin and M. Z. Bazant, Phys. Rev. E **75**, 041301 (2007).
[14] L. Bocquet, A. Colin, and A. Ajdari, Phys. Rev. Lett. **103**, 036001 (2009).
[15] G. Lois and J. M. Carlson, Europhys. Lett. **80**, 58 001 (2007).
[16] G. Picard, A. Ajdari, F. Lequeux, and L. Bocquet, Phys. Rev. E **71**, 010501 (2005).
[17] A. Lemaitre and C. Caroli, Phys. Rev. Lett. **103**, 065501 (2009).
[18] L. Anand, O. Aslan, and S. A. Chester, Int. J. Plast. (to be published).
[19] R. A. B. Engelen, M. G. D. Geers, and F. P. T. Baaijens, Int. J. Plast. **19**, 403 (2003).
[20] L. E. Silbert, D. Ertas, G. S. Grest, T. C. Halsey, D. Levine, and S. J. Plimpton, Phys. Rev. E **64**, 051302 (2001).